Miscibility of Amorphous Solid Dispersions: A Rheological and Solid-state NMR Spectroscopy Study

Sichen Song[1,2], Jianchao Xu[3], Zhenxuan Chen[4], Changquan Calvin Sun[1], Eric J. Munson[3], and Ronald A. Siegel[1,5]**

[1] Department of Pharmaceutics, University of Minnesota, Minneapolis, MN 55455

[2] School of Mathematics, University of Minnesota, Minneapolis, MN 55455

[3] Department of Industrial and Molecular Pharmaceutics, Purdue University, West Lafayette, IN 47907

[4] Analytical Research and Development, Merck & Co., Inc., Rahway, NJ 07065

[5] Department of Biomedical Engineering, University of Minnesota, Minneapolis, MN 55455

[*] Corresponding authors: munsone@purdue.edu (E.J.M.) or siege017@umn.edu (R.A.S.)

ABSTRACT

Miscibility is critical in the prediction of stability against crystallization of amorphous solid dispersions (ASDs) in the solid state. However, currently available approaches for its determination are limited by both theoretical and practical considerations. Recently, a rheological approach guided by the polymer overlap concentration (c^*) has been proposed for miscibility quantification of ASDs [*J. Pharm. Sci.*, 112 (2023) 204−212] and shown to be useful to predict both accelerated and long term physical stability. However, this approach can be only performed at high temperatures (slightly above the melting temperature, T_m, of drugs), and little is known about the difference of miscibility between high and low temperatures (e.g., below the glass transition temperature, T_g). Here we compare miscibility of nifedipine (NIF)/polyvinylpyrrolidone (PVP) ASDs as determined by the rheological approach at 175 °C (~3 °C above T_m of NIF) and solid state NMR (ssNMR) ^{1}H T_1 and $T_{1\rho}$ relaxation times at -20 °C (~66 °C below T_g of NIF). Our results indicate an agreement between the two methods. For low molecular weight (M_w) PVP, $T_{1\rho}$ measurements are more consistent with the rheological approach while T_1 measurements are closer for relatively high M_w PVP. Our findings suggest that the c^* based rheological approach is reliable for directly determining miscibility of deeply cooled ASDs.

GRAPICAL ABSTRACT

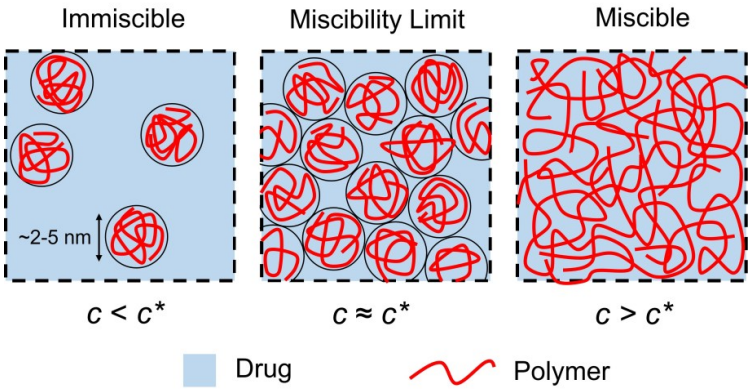

Keywords. Amorphous Solid Dispersions (ASDs), Miscibility, Overlap concentration (c^*), Viscosity, Solid-state NMR, Physical stability.

INTRODUCTION

Amorphization has been established as an increasingly applied formulation strategy to enhance aqueous solubility and dissolution rate of poorly water soluble drugs, since amorphous drug exhibits a higher free energy over its most stable crystalline conterpart.[1,2] However, amorphous materials are thermodynamically unstable and prone to crystalize.[3,4] Amorphous solid dispersions (ASDs), formulated by molecularly dispersing an amorphous drug with a polymer, are used to improve physical stability against crystallization during the shelf life.[5-7]

Although there is no existing first principles mechanism to predict enhanced stability against crystallization of ASDs, some empirical rules have been extensively discussed in the literature, including incorporating high glass transition temperature (T_g) polymers to raise the overall T_g of an ASD leading to lower molecular mobility and segmental dynamics; selecting drug/polymer combinations with relatively strong intermolecular interactions to reduce the thermodynamic driving force and increase the kinetic barrier of crystallization; and combinations of these factors.[8-11] In all cases, it is assumed that miscibility at the molecular level is necessary to achieve desirable physical stability against crystallizaiton.[10,12,13] In this context, miscibility indicates a single homogeneous phase at the molecular level, with physical properties distinct from those of pure components.[12-14] (Although "miscibility" has a classical thermodynamic connotation, in the ASD literature it denotes "homogeneity at the molecular level."[12,15])

The miscibility limit defines the highest drug concentration (or the lowest polymer concentration) above (or below) which an ASD becomes discontinuous with a pure amorphous drug domain and a collection of polymer rich domain.[12]

Currently, the most widely used theoretical scheme for ASD miscibility determination is Flory-Huggins lattice theory.[10,16-19] In this theory, the free energy of mixing per lattice site, F_{mix}, is given by

$$\frac{F_{mix}}{k_B T} = \frac{\phi}{N}\ln\phi + (1-\phi)\ln(1-\phi) + \chi\phi(1-\phi) \quad (1)$$

where k_B is the Boltzmann constant, T is absolute temperature, ϕ is the volume fraction of polymer, N is the ratio of molar volume of the polymer to that of the small molecule drug, and χ is the Flory-Huggins interaction parameter. In this theory, polymer serves as a solvent for drug, and the miscibility limit is identified with the amorphous solubility of drug dissolved in polymer. The drug concentration corresponding to the miscibility limit can be estimated by the intersection of the experimental T_g curve and the spinodal curve,[10] which is obtained by taking the second derivative of Equation 1 with respect to ϕ, where χ is inferred from the following:

$$\left(\frac{1}{T_m^{\text{mix}}} - \frac{1}{T_m^{\text{pure}}}\right) = \frac{-R}{\Delta H_{fus}}\left[\ln(1-\phi) + \left(1-\frac{1}{N}\right)\phi + \chi\phi^2\right] \quad (2)$$

where T_m^{mix} is the depressed melting temperature of crystalline drug/polymer uniform mixtures at high drug loadings, T_m^{pure} is the melting temperature of the pure crystalline drug, R is the gas constant, and ΔH_{fus} is the heat of fusion of the crystalline drug.[18]

However, the accuracy of ASD miscibility determination using Flory-Huggins theory based approach is limited by the following problems. First, the extrapolated χ value from Equation 2 significantly varies under different experimental conditions, such as uniformity and particle size of drug/polymer crystalline mixtures, as well as DSC ramping rate.[20] Theoretically, Flory-Huggins theory assumes that the polymer solution is at equilibrium, hence the result obtained by this approach only directly holds to temperatures close to the melting point (T_m) of the drug. Therefore, miscibility at low temperatures especially below T_g can be predicted only by extrapolation or modeling.[10] Second, Flory-Huggins theory assumes that the polymer solution is a mean field, with a uniform ϕ. This assumption does not hold when the drug loading is sufficiently high (polymer concentration is sufficiently low), since in the dilute limit, the drug/polymer solution is heterogeneous, such that it contains a polymer rich domain within the isolated

77 polymer coils and a pure amorphous drug domain outside the coils (Scheme 1, left).[12] Therefore, Flory-
78 Huggins theory based approach is intrinsically inappropriate to predict the miscibility of high drug loaded
79 ASDs.

80 Recently, Song *et al*. proposed an alternative approach to predict miscibility of ASDs inspired by
81 the overlap concentration (*c**) concept, a critical polymer concentration at which polymer coils start to
82 contact each other (Scheme 1, middle).[12] In this scheme, a small molecule drug serves as solvent for a
83 polymer, which is opposite to the aforementioned Flory-Huggins theory based approach. They found that
84 when polymer concentration is below *c**, ASDs are heterogeneous at the molecular level since it contains
85 two types of domains, namely polymer rich domain and pure amorphous drug domain (Scheme 1, left).
86 For this case, ASD is immiscible. However, when the polymer concentration exceeds *c**, the pure
87 amorphous drug domain is eliminated, and the ASD becomes homogeneous/miscible (Scheme 1, right).
88 The rheologically measured *c** value is estimated as the miscibility limit. Using celecoxib (CEL)/
89 polyvinylpyrrolidone (PVP) and loratadine/PVP ASDs, a strong correlation between *c** and crystallization
90 tendency was found. Remarkably, the *c** based approach predicts not only accelerated physical stability,
91 but also long term stability against crystallization well below T_g. For example, CEL/PVP K12 ASDs with
92 polymer concentrations above *c** remained amorphous for one year storage under ambient conditions,
93 while immiscible CEL/PVP K12 ASDs (PVP K12 concentrations below *c**) crystallized significantly.[12]
94 This approach has been applied to several other drug/polymer combinations and are shown to be robust
95 to predict crystallization tendencies.[21,22]

96 While the aforementioned *c** guided rheological approach has been shown to be useful, there is
97 one more question that needs to be answered: since the *c** value is determined from rheological
98 measurements at high temperature (slightly above T_m of drug), it is assumed that the *c** value remains the
99 same in at low temperatures, i.e., below T_g, due to the rapid quench from the drug/polymer melt, hence
100 polymer conformation does not change significantly. However, this assumption has not yet been verified
101 experimentally.

102 In this work, we report that the miscibility of nifedipine (NIF)/PVP ASDs as measured by the *c**
103 based rheological approach at 175 °C (~3 °C above T_m of NIF) is consistent with that determined by solid-
104 state NMR (ssNMR) spectroscopy ^{1}H $T_{1\rho}$ relaxation times at -20 °C (~66 °C below T_g of NIF). These
105 results confirm that miscibility is determined by the high temperature rheological approach can be directly
106 applied to low temperature stability performance against crystallization. Our finding is relevant to the

rational design of high drug loaded ASD formulations with desirable stability against crystallization during storage.

MATERIALS AND METHODS

Materials. Nifedipine (NIF; OChem Incorporation, protected from light whenever possible) and polyvinylpyrrolidone (PVP; Kollidon® K12, k17, K25; BASF) were used as received. Molecular structures and relevant physical properties of NIF and PVP are shown in Table 1.

Table 1. Molecular Structures and Relevant Physical Properties of NIF and PVP.

	Molecular structure	M_w (g/mol)[1]	$Đ$ (M_w/M_n)*	T_g (°C, onset)	T_m (°C, onset)
NIF	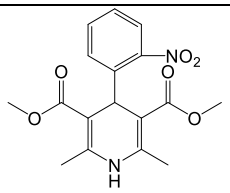	346.3	-	46.5	171.8
PVP K12	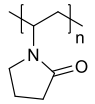	3,800	1.65	102	-
PVP K17		7,300	1.81	138	-
PVP K25		49,500	1.92	165	-

[1] M_w and $Đ$ of PVPs were from the previous work[12].

Methods.

Preparation and characterization of NIF/PVP ASDs. NIF/PVP uniform physical mixtures were prepared by cryogenic milling with a Spex SamplePrep Grinder 6770 (liquid N_2 as coolant). Cryomilling was performed at 10 Hz for five 2 min cycles, each followed by a 2 min cool down. NIF/PVP physical mixtures were then melted at 180 °C for several minutes using a hot plate to ensure complete melting and quenched using liquid N_2. Melt quenched samples were ground manually using a mortar and pestle to reduce particle size and then sieved. Powders of size 250-355 μm were used for ssNMR measurements and physical stability assessment (Figure S1-S2). Differential scanning calorimetry (DSC) was conducted with a TA Q1000 differential scanning calorimeter under continuous helium purge at a flow rate of 25 mL/min. Crystalline NIF and NIF/PVP physical mixtures (4-10 mg) were first heated from 0 °C to 180 °C

at 10 °C/min, jumped to 0 °C, held isothermally for 3 min, and reheated at 10 °C/min to 180 °C. The melting points (endpoint) of NIF with PVP additives were from the first heating cycle, the reported onset T_g values were from the second heating cycle (Table S1).

Miscibility by rheological measurements. Zero shear rate viscosity (η) of pure NIF and NIF/PVP melts was measured using an ARES rheometer. A parallel plate geometry with diameter 25 mm was employed. Briefly, approximately 600 mg of powder was placed on the bottom plate after zero torque, normal force, and gap calibrations. The gap between the parallel plates was approximately 1 mm. Neat NIF and NIF/PVP powders were melted at 175 °C and equilibrated for ~3 min to guarantee complete melting before each measurement. A steady rate sweep test was performed with the initial rate of 1 s^{-1} and the final rate of 100 s^{-1} with continuous N_2 purge at a flow rate of 3 standard cubic feet per minute.

Miscibility determination by Solid-State NMR (ssNMR) ^{1}H T_1 and $T_{1\rho}$ relaxation measurements. All ssNMR spectra were acquired using a Tecmag Redstone HF3 spectrometer operating at 299.62 MHz for ^{1}H and 75.43 MHz ^{13}C (7.0 T static magnetic field). NIF/PVP ASD powders were packed into zirconia rotors and sealed with Kel-F endcaps. Experiments were performed using a Chemagnetics HX probe utilizing 7.5 mm magic angle spinning (MAS) rotors. All ^{13}C spectra were acquired with MAS at 4 kHz,[23] using ramped-amplitude cross polarization (CP),[24] total sideband suppression (TOSS)[25] and SPINAL64 decoupling[26] with a ^{1}H decoupling field of about 62 kHz. A 90° pulse width of about 4 μs and a 1.5 ms contact time were used in all experiments. 3-Methylglutaric acid was used to optimize spectrometer settings and was used as an external standard, with the methyl peak referenced to 18.84 ppm.[27] Temperature settings for the MAS rotor were calibrated using $PbNO_3$[28] and experiments were conducted at -20 °C.

^{1}H T_1 relaxation values were measured using a saturation-recovery experiment through ^{13}C observation. The peak of interest was integrated and plotted against recovery delay times and the values were fitted to the following equation:

$$M = M_0\left(1 - e^{-\tau/T_1}\right) \quad (3)$$

where M is the integrated signal intensity, τ is the recovery delay time, M_0 is an amplitude parameter from the fit, and T_1 is the obtained ^{1}H spin–lattice relaxation time.

^{1}H $T_{1\rho}$ relaxation times were measured by varying the spin-lock duration time following a 90° pulse, followed by cross polarization and ^{13}C detection. A recycle delay of about 3–5 times the measured

^{1}H T_1 was used to maximize the signal-to-noise ratio. A frequency field of about 62 kHz was used for the spin-lock field. The peak of interest was integrated at full width half height and plotted against the variable spin-lock time and the values were fitted to the following equation

$$M = M_0 e^{-\tau/T_{1\rho}} \quad (4)$$

where M is the integrated signal intensity, τ is the spin-lock duration time, M_0 is an amplitude parameter from the fit, and $T_{1\rho}$ is the obtained ^{1}H spin–lattice relaxation time in the rotating frame.

Small Angle X-ray Scattering (SAXS). Synchrotron SAXS experiments were performed at the Sector 5-ID-D beamline (λ = 0.7293 Å) at the Advanced Photon Source, Argonne National Laboratory. Samples were sealed in Tzero aluminum pans under argon. SAXS data was collected on a Rayonix MX 170-HS detector and 8.5 m sample-to-detector distance, giving a range for the scattering vector magnitude q of 2.5 $\times 10^{-3}$ – 0.195 Å. Center and size of Azimuth range are 315° and 120°, respectively. The exposure time was 1 s for each measurement.

RESULTS AND DISCUSSION

Miscibility of ASDs determined by rheological measurement. Before measuring viscosity of NIF/PVP melts, it is necessary to exclude potential phase separation during rheological measurements. We confirmed that NIF is a good solvent for PVP by probing favorable intermolecular interactions. This conclusion was based on the systemic depression of liquidus temperature (T_{liq}, the lowest temperature at which a drug/polymer mixture is a completely liquid) of NIF with an increasing PVP concentration. Figure 1 shows that for NIF doped with PVP K12, T_{liq} decreases with increasing polymer content from neat NIF (177.8 °C), to 18% doped NIF (169.8 °C), and to 30% doped NIF (163.8 °C). This result is consistent with the hydrogen bonding between NIF (dihydropyridine NH group) and PVP (carbonyl group), as determined using ^{13}C ssNMR T_1 relaxation time measurements and Fourier-transform infrared spectroscopy.[9,29]

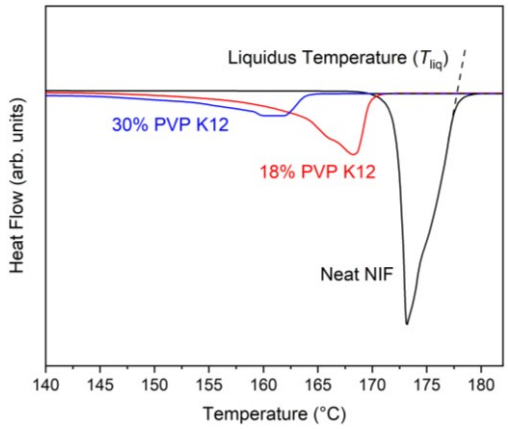

Figure 1. Melting endotherms of neat NIF crystal and NIF/PVP K12 uniform crystalline mixtures.

According to polymer solution theory, polymer solutions in a good solvent can be categorized as three regimes: dilute, semidilute, and concentrated.[30] A dilute solution indicates that the polymer concentration is sufficiently low, that polymer coils are isolated from each other (Scheme 1, left). In this regime, intermolecular interactions between adjacent polymer chains are negligible. The overall viscosity (η) of a dilute polymer solution is linear as a function of polymer concentration (c)

$$\eta = \eta_s(1 + c[\eta]) \quad (5)$$

where η_s is the viscosity of the pure solvent (drug melt) and $[\eta]$ is the intrinsic viscosity of the polymer/solvent pair.[12,30]

As the polymer concentration increases, coils come closer and overlap each other. The critical polymer concentration when polymer coils start to contact is in the semidilute regime and is called overlap concentration, c^* (Scheme 1, middle).[31] Note that c^* can be quite small. It depends on the molecular weight (M_w) since a single polymer coil with a higher M_w pervades a larger volume, therefore, a smaller fraction of polymer (a smaller c^*) is required to occupy the entire space. According to polymer scaling theory, $c^* \sim M_w^{-0.8}$.[31] Therefore, it is easier for polymer coils to strongly overlap at low concentrations. In the semidilite or concentrated regime, since adjacent chains are close and even entangled (Scheme 1, right), the overall viscosity η increases more steeply due to intermolecular interactions and entanglement. Hence, η is no longer a linear function with respect to c. The c^* value (the transition between the dilute and semidilute regions) can be estimated by identifying the crossover between linear and nonlinear regimes in

a viscosity – composition diagram.[12,30] However, there is no general nonlinear equation to describe the behavior of the $\eta - c$ curve in the semidilute and concentrated regimes.[30]

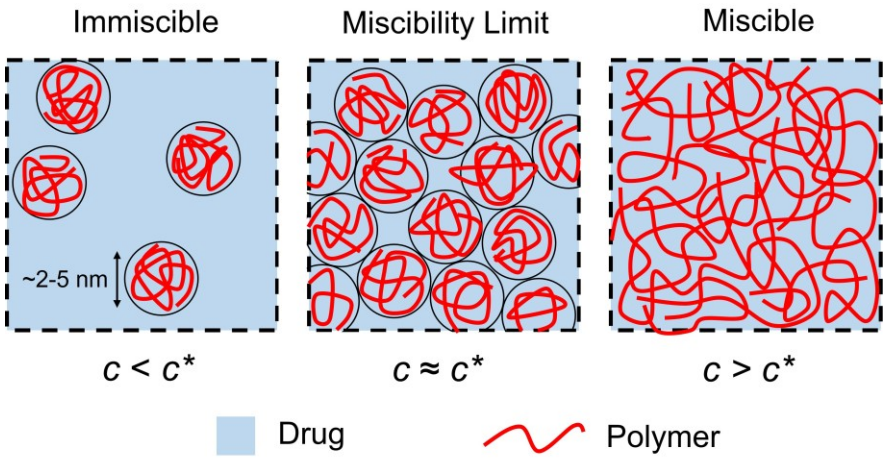

Scheme 1. Scheme of the crossover between dilute (left) and semidilute/concentrated (right) polymer solutions. The light blue background indicates a drug serving as a solvent, and red coils indicate polymers dissolved in amorphous drug.

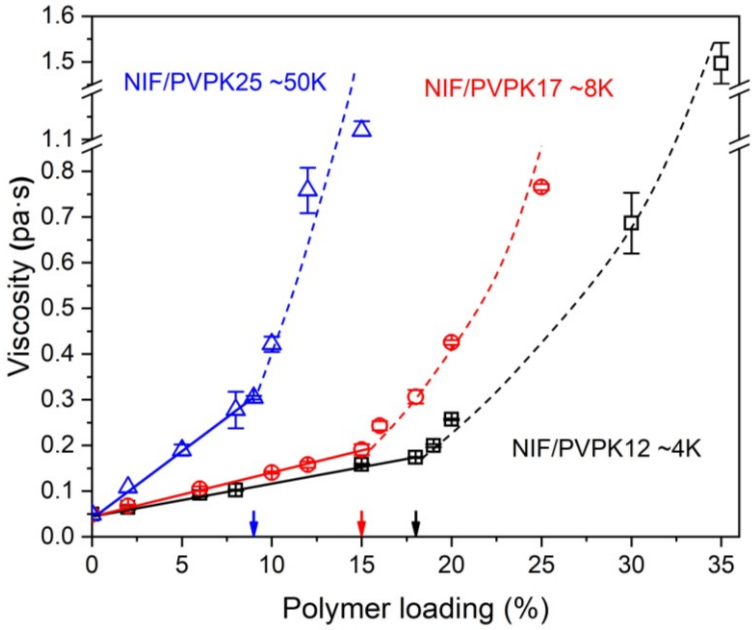

Figure 2. Viscosity-composition diagram of NIF/PVP K12, K17, and K25 at 175 °C. Arrows correspond to c^*, where there is a break in the slopes of the individual viscosity-polymer concentration curves.

Figure 2 summarizes the data collected on the overall viscosity of NIF/PVP melts as a function of PVP concentration at 175 °C, slightly above T_m of NIF, to guarantee a complete melting. For all three with PVPs, M_w ranging from approximately 4,000 to 50,000, when polymer concentration is low, the overall viscosity of NIF/PVP melt increases linearly. Nevertheless, when the polymer concentration is relatively high, the viscosity increases more steeply, the viscosity-composition curve is nonlinear. The c^* values were determined as the location of a change in slope. For NIF/PVP ASDs, c^* values for PVP K12 ($M_w \approx 3{,}800$), PVP K17 ($M_w \approx 7{,}300$), and PVP K25 ($M_w \approx 49{,}500$) are approximately 18, 15, and 9 wt/wt % polymer concentration, respectively. Notice that this change in slope is not sharp (since the transition between dilute and semidilute regions is not a critical phenomenon), and that c^* corresponds to a narrow range of polymer concentrations.

Song *et al.* proposed a potential correlation between the c^* concept and miscibility of ASDs.[12] When the polymer concentration is below c^*, due to the presence of two types of domains: the polymer rich domain within isolated coils and the pure amorphous drug domain outside of polymer coils, a dilute ASD is considered to be heterogenous/immiscible (Scheme 1, left). However, when the polymer concentration is above c^*, the pure amorphous drug domain is eliminated since polymer coils are closely contacted or even entangled, such a semidilute/concentrated ASD is homogeneous/miscible (Scheme 1, right). As the crossover between dilute and semidilute/concentrated regimes, c^* can be assigned as the critical polymer concentration corresponding to the miscibility limit of ASDs (Scheme 1, middle).[12]

We close this section by underlining that the miscibility determinations guided by the c^* concept have been performed only at high temperatures (slightly above T_m of the drug). Next, we shall compare the miscibilities of NIF/PVP ASDs assessed by rheological measurements with those investigated using ssNMR ^{1}H $T_{1\rho}$ relaxation measurements at low temperatures (below T_g) in the next section.

Miscibility of ASDs determined by ssNMR ^{1}H T_1 and $T_{1\rho}$ measurements. ssNMR is an important technique for investigating molecular level miscibility of polymer blends and ASDs.[13,29,32,33] The domain size of drug/polymer miscibility can be determined from ^{1}H T_1 and $T_{1\rho}$ measurements. When drug molecules and polymer chains are closer to each other than the length scale of spin diffusion during a specific time, magnetization transfer between the two components can occur, and the relaxation times of both the drug and polymer are the same and often correspond to the weighted average value of that of the

pure components.[32] If the domain size of the individual components is significantly greater than that of spin diffusion distance during the specified relaxation time, then the relaxation rates are identical to those of the pure components. It is often found that the relaxation rates for the individual components may not be identical, but in between those of the individual components. In this case the components are partially homogenously mixed, and the closer the relaxation times of the individual components, the more homogeneous is the system.

The average domain size of spin diffusion L is determined by

$$\langle L \rangle = \sqrt{6Dt} \quad (6)$$

where D is the spin diffusion coefficient and t is the spin relaxation time. Generally, the value of D is assumed to be 0.1 nm^2/ms.[13] For a typical spin lattice relaxation time ^1H T_1 of 1-5 s, the range of L corresponds to ca. 20-50 nm. For a typical time of spin lattice relaxation in a rotating frame ^1H $T_{1\rho}$ of 5-50 ms, the value of L is between ca. 2 nm and 5 nm. Exact measurement of domain size of ASD miscibility is to some extent uncertain due to the uncertainty of the estimation of D value (It has been suggested that a D value ≤ 0.8 nm^2/ms is acceptable[34]). Nevertheless, ssNMR with spin diffusion measurement provides much higher resolution of miscibility of ASDs than that inferred from conventional analytical techniques such as DSC, Raman mapping, etc.[13,32,33,35,36]

The domain size of miscibility estimated by Equation (6) results in the following three possible scenarios: (1) if the domain size is less than 2-5 nm, both ^1H T_1 and ^1H $T_{1\rho}$ values are identical obtained by amorphous drug and polymer and the ASD is miscible; (2) if the domain size is between 5-20 nm, ^1H T_1 values are identical for drug and polymer but ^1H $T_{1\rho}$ values are different; (3) if the domain size is greater than 20 nm, both ^1H T_1 and ^1H $T_{1\rho}$ values are distinct for drug and polymer. Notice that the prerequisite of this approach is that the relaxation times of pure amorphous drug and polymer should be significantly different. This is indeed the case for the NIF/PVP ASDs. The intrinsic ^1H T_1 and ^1H $T_{1\rho}$ values of neat amorphous NIF (4.2 s and 79.3 ms, respectively) are significantly greater than that of PVP (2.1 s and 27.3 ms, respectively).[13,32] Also, as the system becomes less homogeneous, the difference between the relaxation times will increase towards the relaxation times of the individual components.

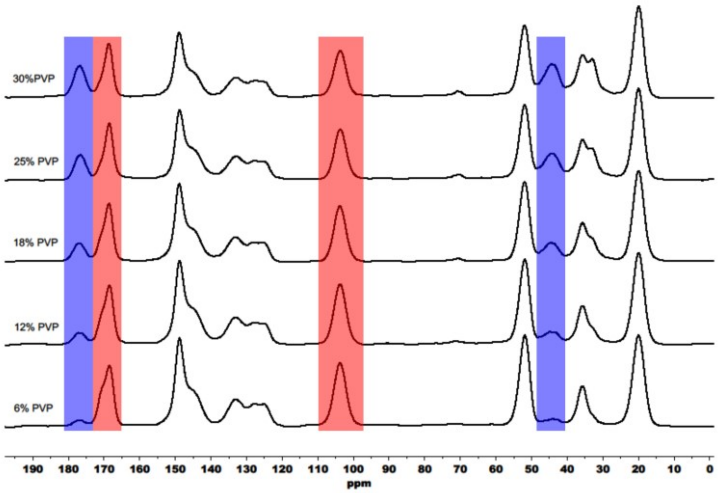

Figure 3. ^{13}C ssNMR spectra of NIF/PVP K12 ASDs. Characteristic peaks of NIF and PVPs are shaded in red and blue, respectively.

Table 1. The measured ^{1}H $T_{1\rho}$ and ^{1}H T_1 values of NIF/PVP K12 ASDs.

			6%	12%	18%	25%	30%
^{1}H $T_{1\rho}$ (ms)	NIF	Peak 1 (103 ppm)	34.13	28.75	24.73	20.33	18.84
		Peak 2 (167 ppm)	32.84	28.02	24.19	21.11	18.05
	PVP K12	Peak 1 (177 ppm)	27.97	26.47	23.35	20.56	17.89
		Peak 2 (43 ppm)	28.48	27.18	23.97	19.56	17.95
^{1}H T_1 (s)	NIF	Peak 1 (103 ppm)	1.499	1.497	1.53	1.447	1.475
		Peak 2 (167 ppm)	1.538	1.514	1.511	1.399	1.463
	PVP K12	Peak 1 (177 ppm)	2.033	1.492	1.563	1.436	1.45
		Peak 2 (43 ppm)	too low	1.508	1.539	1.411	1.537

Figure 3 displays ^{13}C ssNMR spectra of melt quenched NIF/PVP K12 ASDs below, equal to, or above *c**. All spectra exhibit broad peaks, consistent with the amorphous nature as confirmed by XRD immediately before each measurement. Previously, it has been shown that pure amorphous NIF and PVP exhibit single ^{1}H T_1 or ^{1}H $T_{1\rho}$ values, independent of the resonances used for integration.[13] Therefore, any characteristic peak of NIF or PVP that does not overlap with the other component can be used for ^{1}H T_1

and ^{1}H $T_{1\rho}$ relaxation time fitting. Here, the characteristic peaks of NIF at approximately 167 and 103 ppm were selected to determine ^{1}H T_1 or ^{1}H $T_{1\rho}$ values. Similarly, characteristic peaks at around 177 and 43 ppm were used for fitting the ^{1}H T_1 or ^{1}H $T_{1\rho}$ values for PVP, as highlighted in Figure 3. The measured ^{1}H $T_{1\rho}$ and ^{1}H T_1 values of NIF/PVP K12 ASDs are shown in Table 1.

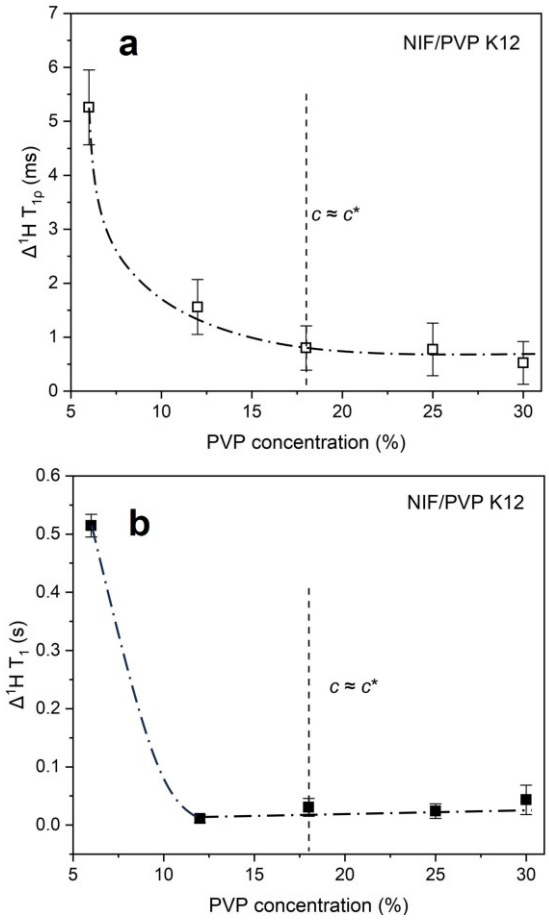

Figure 4. (a) ^{1}H $T_{1\rho}$ and (b) ^{1}H T_1 value difference between NIF and PVP K12 in ASDs as a function of polymer concentration. Dash dot curves are drawn to follow trends of decreasing $\Delta^{1}H$ $T_{1\rho}$ and $\Delta^{1}H$ T_1 values with increasing PVP content.

Since the absolute values of ^{1}H T_1 or ^{1}H $T_{1\rho}$ are sensitive to changes in the moisture content, the differences in ^{1}H T_1 and ^{1}H $T_{1\rho}$ values between NIF and PVP were used to estimate the miscibility of ASDs. Figure 4a shows differences in the ^{1}H $T_{1\rho}$ values between NIF and PVP K12 as a function of polymer concentration. As PVP concentration increases, $\Delta^{1}H$ $T_{1\rho}$ decreases. When the PVP concentration is above c^*, i.e., 18 %, the $\Delta^{1}H$ $T_{1\rho}$ values reach a plateau ($\Delta^{1}H$ $T_{1\rho} \approx 0.7$ ms), which is sufficiently small to conclude that the NIF/PVP K12 ASDs are miscible via ^{1}H $T_{1\rho}$ measurements. On the other hand, when the polymer concentration is below c^*, i.e., 6% and 12%, the $\Delta^{1}H$ $T_{1\rho}$ values indicate that the dilute

NIF/PVP K12 ASDs are no longer homogeneous. Figure 4b shows Δ^1H T_1 values of NIF/PVP K12 ASDs with polymer concentration below, equal, and above c*. The difference from Figure 4a (Δ^1H $T_{1\rho}$ method) is that the Δ^1H T_1 value reaches the plateau when the PVP concentration equals 12%. Therefore, the miscibility limit is approximately 12% by the ^{1}H T_1 measurements. Hence, as suggested by Figure 4, compared to Δ^1H T_1 method, the ^{1}H $T_{1\rho}$ measurements, corresponding to homogeneity over a domain size of 2-5 nm, is more consistent with the rheological approach for determining miscibility of NIF/PVP K12 ASDs.

Comparison between rheological and ssNMR approaches for ASD miscibility determination. The Δ^1H $T_{1\rho}$ measurement provides a better agreement with the c* guided rheological approach to estimate miscibility for NIF/PVP K12 ASDs than does Δ^1H T_1 because the relevant domain size for rheological measurements correspond better to the smaller domain size. This is based on the radius of gyration R_g, of PVP K12 in NIF as determined by SAXS, and Scheme 1. In the Guinier regime, i.e., when $qR_g \leq 1$, the form factor $P(q)$ is given by

$$P(q) \approx 1 - ({R_g}^2/3)q^2 \qquad (7)$$

where q is the momentum transfer vector. Therefore, the value of R_g can be obtained from linear fitting of the plot of $1/I_{ex}$ versus q^2 with a slope ${R_g}^2/3$. Notice that the X-ray scattering intensity I_{ex} is not necessary to be calibrated.[37] Figure 5 plots inverse of I_{ex} of PVP K12 in NIF as a function of q^2. The determined R_g values of PVP K12 is approximately 4 nm.

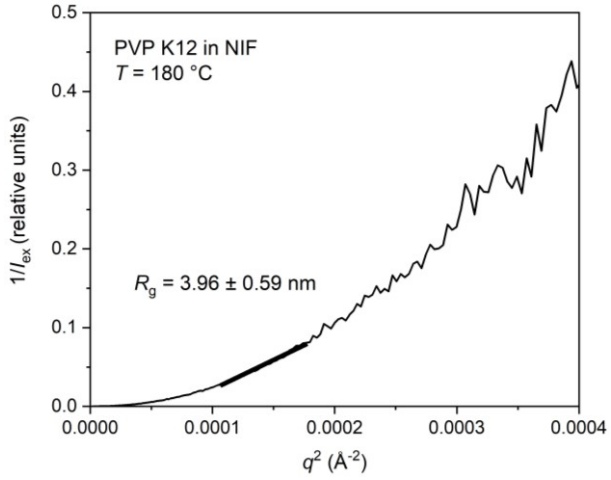

Figure 5. Inverse intensity of X-ray scattering of PVP K12 dissolved in NIF as a function of q^2 at 180 °C.

Because of the comparable size of isolated coils of PVP K12 (~4 nm) and the miscibility domain by the ^{1}H $T_{1\rho}$ measurements (~2-5 nm), when in the dilute regime ($c < c^*$, Scheme 1, left), two types of domains, polymer rich domain (only within isolated coils) and pure amorphous drug domain, can be probed. Therefore, the proton spin diffusion of $T_{1\rho}$ is only effective within the polymer rich domain and the Δ^1H $T_{1\rho}$ between drug and polymer is significantly large. However, when the polymer concentration is above c^* (Scheme 1, right), the latter domain has been eliminated, and the drug and polymer are intimately mixing at the molecular level. Hence, spin diffusion can effectively average the ^{1}H $T_{1\rho}$ values of amorphous drug and polymer, resulting in values that are close to a weighted average of the values for the individual components. A semidilute/concentrated ASD is miscible as estimated by ^{1}H $T_{1\rho}$ measurements. On the other hand, for ^{1}H T_1 measurements, due to the significant difference between the size of the miscibility domain (~20-50 nm) and the isolated PVP K12 coil (~4 nm), ssNMR is expected to probe the pure amorphous drug domain only when the polymer concentration approaches zero ($c \ll c^*$) such that the size of pure amorphous drug domain is comparable or larger than ~20-50 nm, which is consistent with our experimental observations, i.e., the NIF/PVP K12 ASD becomes miscible when the polymer concentration is greater than 12% (less than $c^* \approx 18\%$).

What if the polymer molecular weight (M_w) is relatively high, such that the size of the polymer coil is comparable with that of the miscibility domain by the ^{1}H T_1 measurement (~20-50 nm), as illustrated in Scheme 2? In this case, miscibility quantification by Δ^1H T_1 method should be in consistent with the c^* guided rheological approach. However, since the domain size by ^{1}H $T_{1\rho}$ measurements is much smaller than that of the coil, when $c \approx c^*$, it is comparable with the gap between adjacent coils (Scheme 2). Hence, the miscibility limit determined by Δ^1H $T_{1\rho}$ is expected to be slightly greater than c^*. We tested the above analysis using ssNMR ^{1}H T_1 and $T_{1\rho}$ relaxation times of NIF/PVP K25 ASDs prepared by melt quenching reported by Yuan *et al.*[13] The R_g value of PVP K25 in NIF is estimated as approximately 15 nm according to

$$R_g = \sqrt{Nb^2/6} \quad (8)$$

where N is degree of polymerization (~446) and b is statistical segment length (~16.8 Å).[37] For ^{1}H T_1 measurements, NIF/PVP K25 ASD is miscible when PVP concentration ≥ 10% (immiscible for 95:5 NIF:PVP K25 composition, Figure 6a in the reference[13]). This is consistent with the rheological approach, that the c^* value is determined as 9% (Figure 2). On the other hand, ^{1}H $T_{1\rho}$ values of drug and polymer

342 are significantly different for 5% and 10% polymer concentration NIF/PVP K25 ASDs. It is miscible
343 when the PVP concentration ≥ 25% (Figure 6b in the reference[13]).

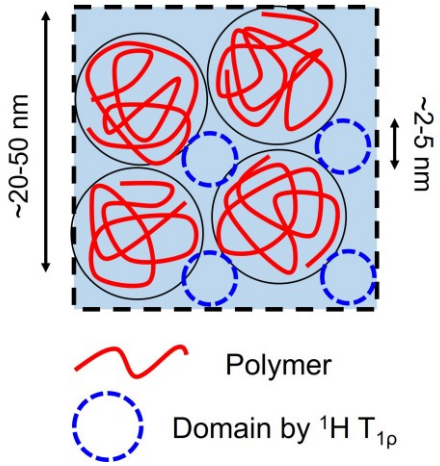

344

345 **Scheme 2.** Illustration of relative size of polymer coil (e.g., PVP K25) and miscibility domain estimated
346 by ssNMR ^{1}H T_1 and $T_{1\rho}$ measurements when $c \approx c^*$.

347

348 **CONCLUSIONS**

349 This work has compared the miscibility of NIF/PVP ASDs prepared by melt quenching, as determined by
350 c^* guided rheological approach at high temperature (slightly above T_m of drug), and ssNMR ^{1}H T_1 and
351 $T_{1\rho}$ measurements at low temperature (well below T_g of drug). In general, these two methods agree with
352 each other. This indicates that miscibility of ASDs as measured using the rheological approach can be
353 directly applied to predict long term stability against crystallization in the glassy state.[12] Specifically, for
354 low molecular weight polymer PVP K12, due to the comparable radius of polymer coil and miscibility
355 domain size by the ^{1}H $T_{1\rho}$ measurements (~2-5 nm), the Δ^1H $T_{1\rho}$ method is consistent with the rheological
356 approach for quantifying ASD miscibility. On the other hand, for relatively higher molecular weight
357 polymer PVP K25, relatively large polymer coil size leads to a better agreement between the rheological
358 approach and the ^{1}H T_1 measurements (~20-50 nm). Future work could compare miscibility of ASDs
359 prepared by melt quench versus spray drying using ssNMR, to determine whether the miscibility
360 prediction by the c^* guided rheological approach can be directly translated to the spray dried ASDs.

361 **ASSOCIATED CONTENT**

Supporting Information. Polarized light microscopy images of NIF/PVP ASDs; T_m and T_g values of neat NIF and NIF/PVPs.

Notes. The authors declare the following competing financial interest(s): E.J.M. is a partial owner of Kansas Analytical Services, a company that provides solid-state NMR services to the pharmaceutical industry. The solid-state NMR results presented here are from academic work at Purdue University, and no data from Kansas Analytical Services are presented.

ACKNOWLEDGMENTS

S.S. thanks Chengbin Huang for helpful discussions, Shuquan Cui for SAXS sample preparations, and David J.W. Grant & Marilyn J. Grant Fellowship for partial financial support. Part of this work was carried out in the College of Science and Engineering Polymer Characterization and Processing Facility, University of Minnesota (UMN), which has received capital equipment funding from the NSF through the UMN MRSEC program under Award Number DMR-2011401. Funding from IPRIME and CIMCEPP is acknowledged.

REFERENCES

1. Newman A, Knipp G, Zografi G 2012. Assessing the performance of amorphous solid dispersions. J Pharm Sci 101(4):1355-1377.
2. Murdande SB, Pikal MJ, Shanker RM, Bogner RH 2010. Solubility advantage of amorphous pharmaceuticals: I. A thermodynamic analysis. J Pharm Sci 99(3):1254-1264.
3. Hancock BC, Shamblin SL, Zografi G 1995. Molecular Mobility of Amorphous Pharmaceutical Solids Below Their Glass Transition Temperatures. Pharm Res 12(6):799-806.
4. Yu L 2001. Amorphous pharmaceutical solids: preparation, characterization and stabilization. Adv Drug Deliv Rev 48(1):27-42.
5. Chiou WL, Riegelman S 1971. Pharmaceutical Applications of Solid Dispersion Systems. J Pharm Sci 60(9):1281-1302.
6. Newman A, Zografi G 2022. What Are the Important Factors That Influence API Crystallization in Miscible Amorphous API–Excipient Mixtures during Long-Term Storage in the Glassy State? Mol Pharmaceutics 19(2):378-391.
7. Newman A, Zografi G 2023. Considerations in the Development of Physically Stable High Drug Load API-Polymer Amorphous Solid Dispersions in the Glassy State. J Pharm Sci 112(1):8-18.
8. Taylor LS, Zografi G 1997. Spectroscopic Characterization of Interactions Between PVP and Indomethacin in Amorphous Molecular Dispersions. Pharm Res 14(12):1691-1698.
9. Kothari K, Ragoonanan V, Suryanarayanan R 2015. The Role of Drug–Polymer Hydrogen Bonding Interactions on the Molecular Mobility and Physical Stability of Nifedipine Solid Dispersions. Mol Pharmaceutics 12(1):162-170.
10. Qian F, Huang J, Hussain MA 2010. Drug–Polymer Solubility and Miscibility: Stability Consideration and Practical Challenges in Amorphous Solid Dispersion Development. J Pharm Sci 99(7):2941-2947.

11. Gui Y, McCann EC, Yao X, Li Y, Jones KJ, Yu L 2021. Amorphous Drug–Polymer Salt with High Stability under Tropical Conditions and Fast Dissolution: The Case of Clofazimine and Poly(acrylic acid). Mol Pharmaceutics 18(3):1364-1372.
12. Song S, Wang C, Zhang B, Sun CC, Lodge TP, Siegel RA 2023. A Rheological Approach for Predicting Physical Stability of Amorphous Solid Dispersions. J Pharm Sci 112(1):204-212.
13. Yuan X, Sperger D, Munson EJ 2014. Investigating Miscibility and Molecular Mobility of Nifedipine-PVP Amorphous Solid Dispersions Using Solid-State NMR Spectroscopy. Mol Pharmaceutics 11(1):329-337.
14. Newman A. 2015. Pharmaceutical Amorphous Solid Dispersions. 1 ed.: Wiley.
15. Dickinson LC, Yang H, Chu CW, Stein RS, Chien JCW 1987. Limits to compatibility in poly(x-methylstyrene)/poly(2,6-dimethylphenylene oxide) blends by NMR. Macromolecules 20(8):1757-1760.
16. Flory PJ 1942. Thermodynamics of High Polymer Solutions. J Chem Phys 10(1):51-61.
17. Huggins ML 1942. Theory of Solutions of High Polymers1. J Am Chem Soc 64(7):1712-1719.
18. Marsac PJ, Shamblin SL, Taylor LS 2006. Theoretical and Practical Approaches for Prediction of Drug–Polymer Miscibility and Solubility. Pharm Res 23(10):2417.
19. Marsac PJ, Li T, Taylor LS 2008. Estimation of Drug–Polymer Miscibility and Solubility in Amorphous Solid Dispersions Using Experimentally Determined Interaction Parameters. Pharm Res 26(1):139.
20. Sun Y, Tao J, Zhang GGZ, Yu L 2010. Solubilities of Crystalline Drugs in Polymers: An Improved Analytical Method and Comparison of Solubilities of Indomethacin and Nifedipine in PVP, PVP/VA, and PVAc. J Pharm Sci 99(9):4023-4031.
21. Sahoo A, Suryanarayanan R, Siegel RA 2020. Stabilization of Amorphous Drugs by Polymers: The Role of Overlap Concentration (*c**). Mol Pharmaceutics 17(11):4401-4406.
22. Sahoo A, Siegel RA 2023. Drug-Polymer Miscibility and the Overlap Concentration (*c**) as Measured by Rheology: Variation of Polymer Structure. Pharm Res 40(9):2229-2237.
23. Andrew ER, Bradbury A, Eades RG 1959. Removal of Dipolar Broadening of Nuclear Magnetic Resonance Spectra of Solids by Specimen Rotation. Nature 183(4678):1802-1803.
24. Pines A, Gibby MG, Waugh JS 2003. Proton‐enhanced NMR of dilute spins in solids. J Chem Phys 59(2):569-590.
25. Dixon WT, Schaefer J, Sefcik MD, Stejskal EO, McKay RA 1982. Total suppression of sidebands in CPMAS C-13 NMR. J Magn Reson (1969) 49(2):341-345.
26. Fung BM, Khitrin AK, Ermolaev K 2000. An Improved Broadband Decoupling Sequence for Liquid Crystals and Solids. J Magn Reson 142(1):97-101.
27. Barich DH, Gorman EM, Zell MT, Munson EJ 2006. 3-Methylglutaric acid as a 13C solid-state NMR standard. Solid State Nucl Magn Reson 30(3):125-129.
28. Bielecki A, Burum DP 1995. Temperature Dependence of207Pb MAS Spectra of Solid Lead Nitrate. An Accurate, Sensitive Thermometer for Variable-Temperature MAS. J magn reson, Ser A 116(2):215-220.
29. Aso Y, Yoshioka S 2006. Molecular mobility of nifedipine−PVP and phenobarbital−PVP solid dispersions as measured by 13C-NMR spin-lattice relaxation time. J Pharm Sci 95(2):318-325.
30. Doi M, Edwards SF. 1986. The Theory of Polymer Dynamics. ed.: Clarendon Press.
31. de Gennes PG. 1979. Scaling Concepts in Polymer Physics. ed.: Cornell University Press.
32. Bovey FA, Mirau PA. 1996. NMR of Polymers. ed.: Academic Press.
33. Duan P, Lamm MS, Yang F, Xu W, Skomski D, Su Y, Schmidt-Rohr K 2020. Quantifying Molecular Mixing and Heterogeneity in Pharmaceutical Dispersions at Sub-100 nm Resolution by Spin Diffusion NMR. Mol Pharmaceutics 17(9):3567-3580.
34. Schmidt-Rohr K, Spiess HW. 1994. Multidimensional Solid-State NMR and Polymers. ed.: Academic Press.
35. Meng F, Dave V, Chauhan H 2015. Qualitative and quantitative methods to determine miscibility in amorphous drug–polymer systems. Eur J Pharm Sci 77:106-111.

36. Newman A, Munson E 2012. Characterizing miscibility in amorphous solid dispersions. Am Pharm Rev 15:92-98.
37. Lodge TP, Hiemenz PC. 2020. Polymer Chemistry. 3 ed.: CRC Press.